Thermal conduction in lattice–matched superlattices of InGaAs/InAlAs

Aditya Sood, Jeremy A. Rowlette, Catherine G. Caneau, Elah Bozorg-Grayeli, Mehdi Asheghi, and Kenneth E. Goodson

Articles you may be interested in

Thermal conduction in lattice–matched superlattices of InGaAs/InAlAs

Aditya Sood,[1,2,a)] Jeremy A. Rowlette,[3] Catherine G. Caneau,[4] Elah Bozorg-Grayeli,[2] Mehdi Asheghi,[2] and Kenneth E. Goodson[2,b)]

[1]*Department of Materials Science and Engineering, Stanford University, Stanford, California 94305, USA*
[2]*Department of Mechanical Engineering, Stanford University, Stanford, California 94305, USA*
[3]*Daylight Solutions, San Diego, California 92128, USA*
[4]*Corning Incorporated, Corning, New York 14831, USA*

Understanding the relative importance of interface scattering and phonon-phonon interactions on thermal transport in superlattices (SLs) is essential for the simulation of practical devices, such as quantum cascade lasers (QCLs). While several studies have looked at the dependence of the thermal conductivity of SLs on period thickness, few have systematically examined the effect of varying material thickness ratio. Here, we study through-plane thermal conduction in lattice-matched $In_{0.53}Ga_{0.47}As/In_{0.52}Al_{0.48}As$ SLs grown by metalorganic chemical vapor deposition as a function of SL period thickness (4.2 to 8.4 nm) and layer thickness ratio (1:3 to 3:1). Conductivities are measured using time-domain thermoreflectance and vary between 1.21 and 2.31 W m^{-1} K^{-1}. By studying the trends of the thermal conductivities for large SL periods, we estimate the bulk conductivities of $In_{0.53}Ga_{0.47}As$ and $In_{0.52}Al_{0.48}As$ to be approximately 5 W m^{-1} K^{-1} and 1 W m^{-1} K^{-1}, respectively, the latter being an order of magnitude lower than theoretical estimates. Furthermore, we find that the Kapitza resistance between alloy layers has an upper bound of ≈ 0.1 m^2 K GW^{-1}, and is negligible compared to the intrinsic alloy resistances, even for 2 nm thick layers. A phonon Boltzmann transport model yields good agreement with the data when the alloy interfaces are modeled using a specular boundary condition, pointing towards the high-quality of interfaces. We discuss the potential impact of these results on the design and operation of high-power QCLs comprised of $In_{1-x}Ga_xAs/In_{1-y}Al_yAs$ SL cores. © 2014 AIP Publishing LLC.
[http://dx.doi.org/10.1063/1.4892575]

The thermal conductivity of superlattices (SLs) determines the figure-of-merit and key operating parameters of several prominent solid state energy conversion and optoelectronic devices.[1–6] Advances in epitaxy have made it possible to grow SLs of a variety of materials with layer thicknesses down to a few nanometers, a length scale comparable to dominant room-temperature phonon mean-free-paths in commonly used semiconductor materials. Measurements of through-plane thermal conductivity, i.e., along the growth direction, have shown a strong reduction from bulk values, by up to an order of magnitude.[7–10] The period thickness d_{SL} can strongly impact the effective thermal conductivity of SLs by increasing the role of interface phonon scattering in the regime of particle-like incoherent transport.[10,11] In the regime of wave-like coherent transport, d_{SL} affects the conductivity through modification of the dispersion relation which can lead to lowering of the group velocity and increasing of mini-Umklapp scattering.[12–15] While most previous studies have looked at the variation of conductivity with total period thickness, there is little systematic data on the impact that the relative material fraction within a period has on the overall conductivity.

Superlattice thermal transport is critically important for mid-infrared and terahertz Quantum Cascade Lasers (QCLs), where efficiencies are limited by large rates of heat generation and high peak operating temperatures.[4] The design of these lasers is hindered at present by the limited experimental thermal property data set for InGaAs/InAlAs SLs. Active cores of QCLs typically consist of aperiodic SL structures with spatially varying layer thicknesses in the range of 2–6 nm.[16] Previous efforts have focused on measuring effective thermal properties of these complex aperiodic structures using techniques such as microprobe photoluminescence[17,18] that give little information about local variations in thermal conductivity within the core. More importantly, these measurements do not separate the thermal resistance of the interfaces from the intrinsic resistance of the alloy layers, and therefore are of limited applicability to building predictive thermal models of QCL active cores with arbitrary stack configurations.

In this paper, we study through-plane thermal conduction in lattice-matched $In_{0.53}Ga_{0.47}As/In_{0.52}Al_{0.48}As$ SLs and its dependence on total period thickness and unit cell alloy thickness ratio. We find that the effective thermal conductivity increases monotonically with increasing fraction of $In_{0.53}Ga_{0.47}As$ and decreases with increasing fraction of $In_{0.52}Al_{0.48}As$. When the thickness ratio is fixed the conductivity does not change appreciably with increasing period thickness. These trends are in good agreement with a Boltzmann transport model employing specular interface conditions, pointing towards the high-quality and low thermal resistance of the interfaces. Additionally, we estimate the bulk conductivity for $In_{0.53}Ga_{0.47}As$ and $In_{0.52}Al_{0.48}As$ to be approximately 5 W m^{-1} K^{-1} and 1 W m^{-1} K^{-1}, respectively.

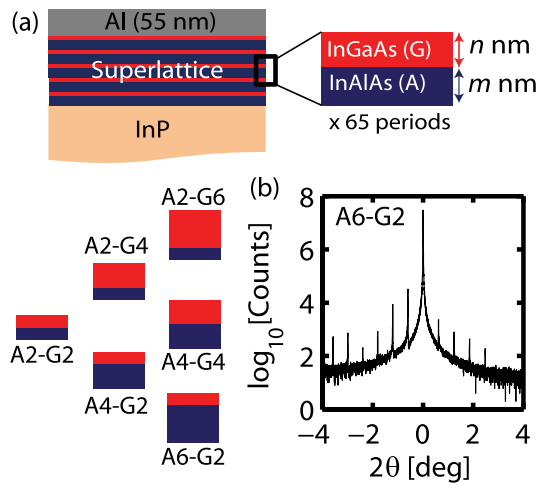a)aditsood@stanford.edu
b)goodson@stanford.edu

FIG. 1. (a) Schematic of superlattice structures. (b) (004) X-ray diffraction pattern of the A6-G2 superlattice, giving a period thickness of 8.49 nm.

A total of six, lattice-matched $In_{0.53}Ga_{0.47}As/In_{0.52}Al_{0.48}As$ SLs, each containing 65 periods, were grown by Metalorganic Chemical Vapor Deposition (MOCVD) on InP substrates (lattice constant $a = 5.88 Å$). These six structures fall into three experimental groups and are herein referred to with a label in the form Am-Gn, where m and n refer to the nominal layer thicknesses of the InAlAs and InGaAs, respectively, in units of nanometers. In Group I, the thickness of InAlAs was fixed at 2 nm while the thickness of InGaAs was varied in steps of 2, 4, 6 nm (Group I = [A2-G2, A2-G4, A2-G6]). In Group II, the thickness of InGaAs was fixed and that of InAlAs was varied in steps of 2, 4, 6 nm (Group II = [A2-G2, A4-G2, A6-G2]). In Group III, the thickness ratio of InAlAs and InGaAs was fixed at 1:1 and the individual layers were doubled from 2 to 4 nm (Group III = [A2-G2, A4-G4]). Note the intersection of all three groups with A2-G2 to yield a total of six unique structures. A summary of the structure designs is shown in Figure 1, along with a representative X-ray diffraction (XRD) spectrum taken on sample A6-G2, showing the high quality of growth. XRD was used to measure exact period thicknesses at multiple points on each wafer (see Table I). A detailed mapping of A2-G2 showed a period of (4.18 ± 0.05) nm over the 2″ diameter wafer, excluding a 3 mm periphery zone.

Through-plane thermal conductivity was measured using time-domain thermoreflectance (TDTR), a well-established pump-probe technique.[19–22] A 55 nm thick aluminum transducer film was deposited on each sample by electron-beam evaporation in a common deposition run. $1/e^2$ pump and probe spot sizes of 10 μm and 6 μm, respectively, were used in these experiments. Pump pulses were amplitude modulated at a frequency $f_{mod} = 2$ MHz for lock-in detection. Measurements were performed at three randomly selected locations on each sample, with four traces recorded per spot. The systematic relative error between each of the four traces taken at the same location was substantially below the intrinsic noise floor of the measurement and was therefore undetectable. The average signal to noise ratio was 200:1, at a probe delay time of 1 ns with a lock-in time constant of 10 ms. The averaged data of the 12 measurements per sample were analyzed using a multilayer heat diffusion model.

The through-plane thermal conductivity of the SL (κ_{SL}) and the thermal boundary resistance (TBR) between the Al transducer and SL film (TBR_{Al-SL}) [Table I] were extracted simultaneously by fitting the data using a least squares algorithm. The measured κ_{SL} varied by ~2% across multiple spots on each sample, which is smaller than the error bars propagated by uncertainties in the values of the fixed parameters, predominantly the thickness of the aluminum layer (± 2 nm) and the specific heat of the SL, C_{SL} ($\pm 5\%$) (see supplementary material[22]). The latter was nominally taken to be a thickness weighted average of the specific heats of the alloys InGaAs and InAlAs, which were found by linearly interpolating between the binary compounds InAs, GaAs and AlAs.[23] The measurement is insensitive to the TBR at the SL film–InP substrate interface, and the in-plane thermal conductivity of the SL.

In Figure 2(a), we plot κ_{SL} as a function of the SL period thickness. We find that κ_{SL} increases with d_{SL} for the Group I SLs, i.e., the conductivity increases with period thickness when the thickness of the InAlAs layer is fixed, while that of the InGaAs is allowed to vary. On the other hand, we observe a decreasing trend in κ_{SL} versus d_{SL} for the Group II SLs,

TABLE I. Superlattice sample properties and TDTR data.

Sample	d_{SL}[a] (nm)	d_{film}[b] (nm)	C_{SL} ($\times 10^6$ J m^{-3} K^{-1})	κ_{SL} (W m^{-1} K^{-1})	TBR_{Al-SL} (m^2 K GW^{-1})
A2-G2	4.18	271.7	1.889	1.63 ± 0.09	13.7 ± 0.6
A2-G4	6.28	408.2	1.883	1.88 ± 0.12	12.1 ± 0.6
A4-G2	6.35	412.8	1.894	1.50 ± 0.11	12.4 ± 0.6
A2-G6	8.38	544.7	1.881	2.31 ± 0.18	10.6 ± 0.5
A6-G2	8.49	551.9	1.896	1.21 ± 0.12	12.0 ± 0.4
A4-G4	8.44	548.6	1.889	1.66 ± 0.15	12.2 ± 0.5

[a]d_{SL} is the thickness of one period measured by XRD.
[b]d_{film} is the total SL film thickness, consisting of 65 periods.
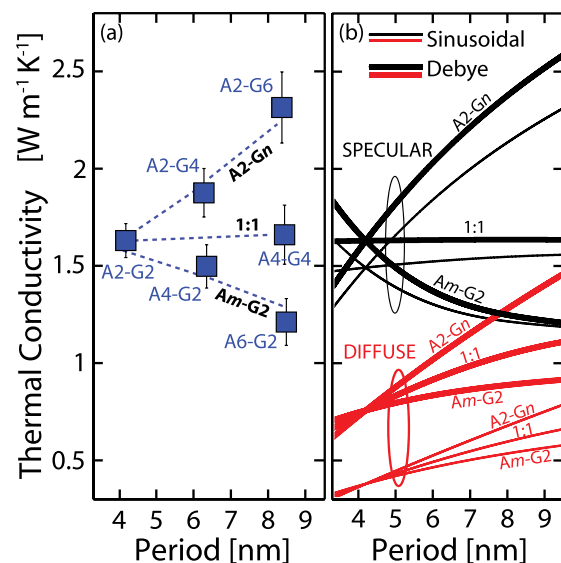

FIG. 2. (a) Through-plane thermal conductivity plotted versus period thickness. Blue dotted lines are guides to the eye, showing trends for A2-Gn, Am-G2, and 1:1 SLs. (b) BTE predictions for two extreme cases of interface scattering: fully specular (black) and fully diffuse (red), for two different phonon dispersions (heavy lines—Debye, light lines—sinusoidal).

implying that the addition of InAlAs to a SL period decreases the conductivity when the thickness of the InGaAs is held constant. Finally, we find that the two SLs in Group III that have the same ratio of layer thicknesses, A2-G2 and A4-G4 have nearly equal conductivity to within experimental error bars. κ_{SL} therefore depends both on the total SL period thickness and the intra-period ratio of layer thicknesses. Simple arguments based on a series resistance model under the assumption of thickness independent layer conductivities suggest that the TBR between the InGaAs and InAlAs would need to be negligibly small in order to explain the trends in the data. In such a scenario, doubling d_{SL} while maintaining the same ratio of layer thicknesses would exactly double the thermal resistance per period, keeping κ_{SL} unchanged. An estimate of the thermal resistance due to a single InGaAs/InAlAs interface can be obtained by extrapolating the single

period SL resistances of A2-G2 and A4-G4 down to zero period thickness, giving an upper bound of close to $0.1\,\mathrm{m^2\,K\,GW^{-1}}$. However, such arguments need to be applied with caution, as the layer thicknesses involved here are in the 2–6 nm range, length-scales that are comparable with dominant phonon mean free paths in InGaAs and InAlAs.

In order to establish a rigorous model for thermal conduction within the sub-continuum regime that accounts for size effects and phonon interface transmission, we develop Boltzmann transport equation (BTE) simulations. Using a framework outlined by Chen,[10] we solve the BTE in order to calculate the effective through-plane thermal conductivity of the SL.

Under the single mode relaxation time approximation, the solution to the BTE within layer i of a SL repeating unit cell ($i = 1, 2$) for phonons of frequency ω is given by[10]

$$g_{i,\omega}(z_i,\mu_i) = \begin{cases} g_{iL,\omega}^{+}(0,\mu_i)e^{-\frac{z_i}{\Lambda_{i,\omega}\mu_i}} - \int_{\eta_i=0}^{z_i}\frac{\partial f_{0i,\omega}}{\partial \eta_i}e^{-\frac{z_i-\eta_i}{\Lambda_{i,\omega}\mu_i}}d\eta_i, & \mu_i \in (0,1) \\[2mm] g_{iR,\omega}^{-}(L_i,-|\mu_i|)e^{\frac{z_i-L_i}{\Lambda_{i,\omega}|\mu_i|}} + \int_{\eta_i=z_i}^{L_i}\frac{\partial f_{0i,\omega}}{\partial \eta_i}e^{\frac{z_i-\eta_i}{\Lambda_{i,\omega}|\mu_i|}}d\eta_i, & \mu_i \in (-1,0) \end{cases} \quad (1)$$

where $g_{i,\omega}(z_i,\mu_i) = f_{i,\omega}(z_i,\mu_i) - f_{0i,\omega}(z_i)$ is the departure from equilibrium of the phonon population at a coordinate z_i, along a line that makes a direction cosine of μ_i with the film-normal direction, and $g_{iL,\omega}^{+}(0,\mu_i)$ and $g_{iR,\omega}^{-}(L_i,-|\mu_i|)$ are boundary values of $g_{i,\omega}$ at the left and right interfaces of the ith layer, respectively. $f_{0i,\omega}$ is the equilibrium Bose-Einstein distribution function, $\Lambda_{i,\omega}$ is the phonon mean free path, and L_i is the thickness of the layer.

The interface phonon populations within adjacent layers are related by applying detailed balance across the interface, accounting for partial transmission and reflection of phonons traveling in different directions, as follows:

$$f_{1,\omega}^{-}(L_1,-\mu_1) = p\left[\gamma_{s,12,\omega}f_{1,\omega}^{+}(L_1,\mu_1) + \tau_{s,21,\omega}\right.$$
$$\left. \times \frac{v_{2,\omega}D_{2,\omega}}{v_{1,\omega}D_{1,\omega}}f_{2,\omega}^{-}(0,-\mu_2)\frac{\mu_2 d\mu_2}{\mu_1 d\mu_1}\right]$$
$$+ 2(1-p)\left[\gamma_{d,12,\omega}\int_0^1 f_{1,\omega}^{+}(L_1,\mu_1)\mu_1 d\mu_1\right.$$
$$\left. + \tau_{d,21,\omega}\frac{v_{2,\omega}D_{2,\omega}}{v_{1,\omega}D_{1,\omega}}\int_0^1 f_{2,\omega}^{-}(0,-\mu_2)\mu_2 d\mu_2\right],$$
$$(2)$$

where p is the specularity parameter denoting the fraction of phonons that undergo specular reflection and transmission, $v_{i,\omega}$ is the phonon group velocity, and $D_{i,\omega}$ is the density of states.

Similar equations apply at each of the three other interfaces within a SL period, i.e., for $f_{1,\omega}^{+}(0,\mu_1)$, $f_{2,\omega}^{+}(0,\mu_2)$, and $f_{2,\omega}^{-}(L_2,-\mu_2)$.

The transmission coefficients for diffuse scattering (τ_d) are given by the Diffuse Mismatch Model (DMM): $\tau_{d,12,\omega}$

$= v_{2,\omega}D_{2,\omega}/[v_{1,\omega}D_{1,\omega} + v_{2,\omega}D_{2,\omega}]$, while those for specular scattering (τ_s) are given by the Acoustic Mismatch Model (AMM):[24] $\tau_{s,12,\omega}(\mu_1) = 4Z_{1,\omega}Z_{2,\omega}\mu_1\mu_2/(Z_{1,\omega}\mu_1 + Z_{2,\omega}\mu_2)^2$, where $Z_{i,\omega} = \rho_i v_{i,\omega}$ is the acoustic impedance. Reflection coefficients γ_s and γ_d are calculated from the transmission coefficients under conditions of energy conservation, i.e., $\gamma_{d,12,\omega} = 1 - \tau_{d,12,\omega}$ and $\gamma_{s,12,\omega}(\mu_1) = 1 - \tau_{s,12,\omega}(\mu_1)$.

In the absence of heat generation, periodicity of the SL is imposed by requiring that the angular distribution of the departure function be equal at equivalent coordinates inside every SL unit cell (see Chen[10]): $g_{i,\omega}(z_i,\mu_i) = g_{i_N,\omega}(z_{i_N},\mu_{i_N})$, where i_N denotes layer i of the adjacent super cell.

These equations are solved numerically until convergence is achieved, i.e., heat flux is conserved. The total heat flux q_z is found by integrating the normal component of the energy flux over all angles and across the full spectrum of phonon frequencies and polarization modes M

$$q_z = \frac{1}{2}\sum_M \int_{\omega=0}^{\omega_{c,i}} v_{i,\omega}\hbar\omega D_{i,\omega}\int_{\mu_i=-1}^{1} g_{i,\omega}(z_i,\mu_i)\mu_i d\mu_i \, d\omega. \quad (3)$$

The effective SL conductivity κ_{SL} is given by $q_z/\overline{\nabla T}$ where $\overline{\nabla T}$ is the spatially averaged temperature gradient over one SL period.

A full calculation of κ_{SL} requires knowledge of the phonon dispersion and scattering rates in bulk materials InGaAs and InAlAs. In this paper, we consider two different cases for the phonon dispersion. In one case, we assume a Debye model[25] with acoustic sound speeds in the alloys given by a linear interpolation $v_{LA/TA,In(Ga/Al)As} = (0.47)v_{LA/TA,(Ga/Al)As} + (0.53)v_{LA/TA,InAs}$.[26] Values of $v_{LA/TA}$ for the binary compounds are found from calculated dispersion curves in the [100] direction[27,28] taking the slopes in the limit $\omega \to 0$. In

the second case, we consider a sinusoidal dispersion: $\omega = \omega_c \sin(\pi k / 2 k_0)$, where $k_0 = 2\pi/a$, with the low frequency group velocity given by the sound speed of the Debye model. In both cases, phonon scattering processes are modeled using a frequency and polarization independent bulk mean free path $\Lambda_{b,i}$, i.e., in the grey medium approximation. The bulk conductivity $\kappa_{b,i}$ is given by $\kappa_{b,i} = [\int_{LA} \xi_{i,\omega} v_{i,\omega} d\omega + 2\int_{TA} \xi_{i,\omega} v_{i,\omega} d\omega] \Lambda_{b,i}/3$, where $\xi_{i,\omega}$ denotes the specific heat per unit angular frequency. The model explicitly neglects any optical phonon contributions to heat conduction due to their small group velocities. First principles calculations in GaAs have shown that although optical phonons can affect thermal conductivity indirectly through acoustic-optical scattering channels, more than 90% of the heat is conducted by acoustic phonons at room temperature.[29]

In order to estimate the dominant bulk mean free path, we use the bulk conductivity values of $\kappa_{b,InGaAs} = 5 \, \mathrm{W\,m^{-1}\,K^{-1}}$ and $\kappa_{b,InAlAs} = 1.2 \, \mathrm{W\,m^{-1}\,K^{-1}}$. While the conductivity of InGaAs is based on experimental data from literature,[30] no such data have been reported for InAlAs. Our estimate of $1.2 \, \mathrm{W\,m^{-1}\,K^{-1}}$ is based on the asymptotic value of the thermal conductivity of A*m*-G2 SLs at large period thicknesses. We note that this experimental value is lower than that estimated using a semi-empirical alloy disorder model,[31] which gives $\sim 17 \, \mathrm{W\,m^{-1}\,K^{-1}}$. This suggests that the simplified alloy scattering picture might not be sufficient to explain the low thermal conductivity of InAlAs.

Using the above values for $\kappa_{b,i}$ and other parameters listed in Table II, we estimate grey phonon mean free paths of $\Lambda_{b,InGaAs} = 5.8 \, \mathrm{nm}$, $\Lambda_{b,InAlAs} = 1.3 \, \mathrm{nm}$, and $\Lambda_{b,InGaAs} = 15 \, \mathrm{nm}$, $\Lambda_{b,InAlAs} = 3.5 \, \mathrm{nm}$ for the Debye and sinusoidal dispersion models, respectively. Finally, we assume that no phonon mode conversion takes place at the interfaces, and that scattering is purely elastic for the specular case. Figure 2(b) shows the predictions of this model (for $p = 1$, i.e., fully specular, and $p = 0$, i.e., fully diffuse cases).

For both types of phonon dispersion, the qualitative trends predicted by the models are similar. They predict that when the interfaces are fully diffuse, κ_{SL} increases with d_{SL} for all groups of SLs, i.e., Group I [A2-G*n* (*n* = 2, 4, 6)], Group II [A*m*-G2 (*m* = 2, 4, 6)], and Group III [A*m*-G*n* (*m* = *n*)]. This type of behavior is similar to what would be obtained using a series resistor model with non-negligible TBR at the interfaces. In contrast, when the interfaces are fully specular, the dependence of κ_{SL} on d_{SL} is different for the three groups. κ_{SL} increases with d_{SL} for Group I SLs, tending towards the bulk conductivity of InGaAs for large

periods, while the opposite happens for Group II SLs, which show a decreasing trend due to the lower bulk conductivity of InAlAs. Furthermore, the specular model predicts nearly equal conductivities of the 1:1 SLs A2-G2 and A4-G4. Overall, the BTE simulations predict the correct trends in κ_{SL} versus d_{SL} for all three SL groups, for both the Debye and sinusoidal dispersion models, when interface scattering is fully specular. The predictions are also robust to perturbations in the assumed bulk conductivities (See supplementary materials[22]).

The specularity parameter p is a function of the relative magnitudes of two length scales, the dominant phonon wavelength (λ) and the interface roughness (σ).[32] An interface that is rough ($\lambda \ll \sigma$) has a largely diffuse, and one that is smooth ($\lambda \gg \sigma$) a largely specular character. The former scatters incident phonons randomly in all directions, with an isotropic transmission probability within each medium, leading to a larger value of TBR than in the purely specular case. Also for materials that are acoustically similar, which is likely the case in InGaAs and InAlAs, specular interfaces show near unity transmission probability based on the AMM, which results in a TBR that is negligibly small compared to the intrinsic layer resistances. Therefore, the good agreement between the data and specular BTE model supports our earlier hypothesis of a small TBR based on the series resistance model.

Recent studies have shown the effects of coherent phonon heat conduction in SL structures, where it is important to consider wave-like effects such as phonon interference.[15] In such cases, the SL is best modeled as a material with an effective dispersion that depends on the period thickness. While we do not rule out the possibility of such effects here, we believe that the current model sufficiently captures the essential physics at play, reproducing the trends observed in the data. Studies at low temperatures may provide additional insights into coherent phonon behavior. We also note that recent literature has shown that scattering of long wavelength phonons at SL film boundaries can cause κ_{SL} to depend not only on d_{SL} but also on the total SL film thickness, d_{film}.[25,33] In such a case, κ_{SL} saturates when d_{film} exceeds the mean free path of the dominant heat conducting coherent-ballistic phonons. In the pure binary GaAs/AlAs SL system,[33] a film thickness of $\sim 220 \, \mathrm{nm}$ was shown to be sufficient for κ_{SL} to saturate to an intrinsic value at room temperature. In comparison, we expect this saturation to occur at significantly smaller film thicknesses in the strongly alloyed InGaAs/InAlAs system. Given that the film

TABLE II. BTE model parameters.

| Material | | $v_{\omega=0}$ ($\times 10^3$ ms^{-1}) | ω_c[a] ($\times 10^{13}$ rad s^{-1}) | | $C_{ac,Deb}$[b] ($\times 10^5$ J m^{-3} K^{-1}) | κ_b (W m^{-1} K^{-1}) | Λ_b (nm) | |
			Deb.	Sine.			Deb.	Sine.
InGaAs	LA[c]	4.40	4.64	2.99	2.56	5.0	5.8	15
	TA[c]	2.70	2.85	1.84	2.67			
InAlAs	LA	4.77	5.04	3.24	2.53	1.2	1.3	3.5
	TA	2.96	3.12	2.01	2.66			

[a]ω_c is the cutoff frequency $= (24\pi^2)^{1/3} v_{\omega=0}/a$ for Debye, $= 4 v_{\omega=0}/a$ for sinusoidal.
[b]$C_{ac,Deb}$ is the Debye specific heat of acoustic phonons.
[c]LA and TA refer to longitudinal and transverse acoustic branches, respectively.

thicknesses used in this study are greater than 270 nm, the role of size effects is unlikely.

The data and model together illustrate the roles of intrinsic versus interface phonon scattering in SLs of InGaAs/InAlAs. We have shown that the interfaces must have a high degree of specularity in order to produce divergent trends for the through-plane conductivity as a function of period thickness, pointing towards the excellent quality of interfaces in this lattice-matched system. Further, it is important to consider the relative thicknesses of the constituent layers within a SL when drawing a relationship between through-plane thermal conductivity and period thickness. This is especially so when the materials are closely matched, and the interfaces are highly transmitting.

Our measurements also provide relevant data for the layer thickness dependent thermal conductivity in the technologically important InGaAs/InAlAs system, showing that the local thermal resistance can vary greatly depending on the exact layer configuration. With special relevance to QCLs, we have examined the fundamental factors that limit heat conduction using a physically rigorous phonon transport model and have shown that high-quality interfaces do not play a significant role in impeding through-plane thermal conduction in this lattice-matched system. The data and theoretical analysis together enable the possibility of building accurate models for thermal conduction within active cores of QCLs with arbitrary stack geometry. Incorporating such models within the design process of QCL devices would potentially lead to structures with optimized thermal performance, improved overall wall plug efficiency and optical mode stability.

[1]B. S. Williams, Nat. Photonics **1**, 517 (2007).
[2]F. Xie, C. Caneau, H. P. Leblanc, N. J. Visovsky, S. C. Chaparala, O. D. Deichmann, L. C. Hughes, C. Zah, D. P. Caffey, and T. Day, IEEE J. Sel. Top. Quantum Electron. **17**, 1445 (2011).
[3]F. Xie, C. G. Caneau, H. P. LeBlanc, N. J. Visovsky, S. Coleman, L. C. Hughes, and C. Zah, Appl. Phys. Lett. **95**, 091110 (2009).
[4]S. S. Howard, Z. Liu, D. Wasserman, A. J. Hoffman, T. S. Ko, and C. F. Gmachl, IEEE J. Sel. Top. Quantum Electron. **13**, 1054 (2007).
[5]I. Chowdhury, R. Prasher, K. Lofgreen, G. Chrysler, S. Narasimhan, R. Mahajan, D. Koester, R. Alley, and R. Venkatasubramanian, Nat. Nanotechnol. **4**, 235 (2009).
[6]X. Fan, G. Zeng, C. LaBounty, J. E. Bowers, E. Croke, C. C. Ahn, S. Huxtable, A. Majumdar, and A. Shakouri, Appl. Phys. Lett. **78**, 1580 (2001).
[7]W. Capinski, H. Maris, T. Ruf, M. Cardona, K. Ploog, and D. Katzer, Phys. Rev. B **59**, 8105 (1999).
[8]S.-M. Lee, D. G. Cahill, and R. Venkatasubramanian, Appl. Phys. Lett. **70**, 2957 (1997).
[9]R. Venkatasubramanian, Phys. Rev. B **61**, 3091 (2000).
[10]G. Chen, Phys. Rev. B **57**, 14958 (1998).
[11]G. Chen and M. Neagu, Appl. Phys. Lett. **71**, 2761 (1997).
[12]M. Simkin and G. Mahan, Phys. Rev. Lett. **84**, 927 (2000).
[13]G. Chen, J. Heat Transfer **121**, 945 (1999).
[14]S. Y. Ren and J. D. Dow, Phys. Rev. B **25**, 3750 (1982).
[15]J. Ravichandran, A. K. Yadav, R. Cheaito, P. B. Rossen, A. Soukiassian, S. J. Suresha, J. C. Duda, B. M. Foley, C.-H. Lee, Y. Zhu, A. W. Lichtenberger, J. E. Moore, D. A. Muller, D. G. Schlom, P. E. Hopkins, A. Majumdar, R. Ramesh, and M. A. Zurbuchen, Nat. Mater. **13**, 168 (2014).
[16]A. Lops, V. Spagnolo, and G. Scamarcio, J. Appl. Phys. **100**, 043109 (2006).
[17]V. Spagnolo, M. Troccoli, G. Scamarcio, C. Gmachl, F. Capasso, A. Tredicucci, A. M. Sergent, A. L. Hutchinson, D. L. Sivco, and A. Y. Cho, Appl. Phys. Lett. **78**, 2095 (2001).
[18]M. S. Vitiello, G. Scamarcio, and V. Spagnolo, IEEE J. Sel. Top. Quantum Electron. **14**, 431 (2008).
[19]M. A. Panzer, M. Shandalov, J. A. Rowlette, Y. Oshima, P. C. McIntyre, and K. E. Goodson, IEEE Electron Device Lett. **30**, 1269 (2009).
[20]J. P. Reifenberg, M. A. Panzer, J. A. Rowlette, M. Asheghi, H.-S. P. Wong, and K. E. Goodson, IEEE Electron Device Lett. **31**, 56 (2010).
[21]J. A. Rowlette, Ph.D. thesis, Stanford University, 2010.
[22]See supplementary material at http://dx.doi.org/10.1063/1.4892575 for details on our TDTR setup, experimental sensitivity plots and error propagation, and a perturbative analysis of the BTE model.
[23]S. Adachi, *Properties of Semiconductor Alloys: Group-IV, III-V and II-VI Semiconductors* (John Wiley & Sons, 2009).
[24]E. Swartz and R. Pohl, Rev. Mod. Phys. **61**, 605 (1989).
[25]R. Cheaito, J. C. Duda, T. E. Beechem, K. Hattar, J. F. Ihlefeld, D. L. Medlin, M. A. Rodriguez, M. J. Campion, E. S. Piekos, and P. E. Hopkins, Phys. Rev. Lett. **109**, 195901 (2012).
[26]S. Adachi, J. Appl. Phys. **58**, R1 (1985).
[27]P. Giannozzi, S. de Gironcoli, P. Pavone, and S. Baroni, Phys. Rev. B **43**, 7231 (1991).
[28]F. Zhou, A. L. Moore, J. Bolinsson, A. Persson, L. Fröberg, M. T. Pettes, H. Kong, L. Rabenberg, P. Caroff, D. A. Stewart, N. Mingo, K. A. Dick, L. Samuelson, H. Linke, and L. Shi, Phys. Rev. B **83**, 205416 (2011).
[29]T. Luo, J. Garg, J. Shiomi, K. Esfarjani, and G. Chen, Europhys. Lett. **101**, 16001 (2013).
[30]S. Adachi, J. Appl. Phys. **54**, 1844 (1983).
[31]S. Adachi, J. Appl. Phys. **102**, 063502 (2007).
[32]J. M. Ziman, *Electrons and Phonons: The Theory of Transport Phenomena in Solids* (Oxford University Press, 2001), pp. 250–255.
[33]M. N. Luckyanova, J. Garg, K. Esfarjani, A. Jandl, M. T. Bulsara, A. J. Schmidt, A. J. Minnich, S. Chen, M. S. Dresselhaus, Z. Ren, E. A. Fitzgerald, and G. Chen, Science **338**, 936 (2012).